Available online at www.sciencedirect.com
ScienceDirect
Journal of volcanology and geothermal research
Journal of Volcanology and Geothermal Research 160 (2007) 285–299
www.elsevier.com/locate/jvolgeores

Array analyses of volcanic earthquakes and tremor recorded at Las Cañadas caldera (Tenerife Island, Spain) during the 2004 seismic activation of Teide volcano

Javier Almendros *, Jesús M. Ibáñez, Enrique Carmona, Daria Zandomeneghi

Instituto Andaluz de Geofísica, Universidad de Granada, 18071 — Granada, Spain

Received 3 March 2006; received in revised form 29 August 2006; accepted 4 October 2006
Available online 22 November 2006

Abstract

We analyze data from three seismic antennas deployed in Las Cañadas caldera (Tenerife) during May–July 2004. The period selected for the analysis (May 12–31, 2004) constitutes one of the most active seismic episodes reported in the area, except for the precursory seismicity accompanying historical eruptions. Most seismic signals recorded by the antennas were volcano-tectonic (VT) earthquakes. They usually exhibited low magnitudes, although some of them were large enough to be felt at nearby villages. A few long-period (LP) events, generally associated with the presence of volcanic fluids in the medium, were also detected. Furthermore, we detected the appearance of a continuous tremor that started on May 18 and lasted for several weeks, at least until the end of the recording period. It is the first time that volcanic tremor has been reported at Teide volcano. This tremor was a small-amplitude, narrow-band signal with central frequency in the range 1–6 Hz. It was detected at the three antennas located in Las Cañadas caldera. We applied the zero-lag cross-correlation (ZLCC) method to estimate the propagation parameters (back-azimuth and apparent slowness) of the recorded signals. For VT earthquakes, we also determined the S–P times and source locations. Our results indicate that at the beginning of the analyzed period most earthquakes clustered in a deep volume below the northwest flank of Teide volcano. The similarity of the propagation parameters obtained for LP events and these early VT earthquakes suggests that LP events might also originate within the source volume of the VT cluster. During the last two weeks of May, VT earthquakes were generally shallower, and spread all over Las Cañadas caldera. Finally, the analysis of the tremor wavefield points to the presence of multiple, low-energy sources acting simultaneously. We propose a model to explain the pattern of seismicity observed at Teide volcano. The process started in early April with a deep magma injection under the northwest flank of Teide volcano, related to a basaltic magma chamber inferred by geological and geophysical studies. The stress changes associated with the injection produced the deep VT cluster. In turn, the occurrence of earthquakes permitted an enhanced supply of fresh magmatic gases toward the surface. This gas flow induced the generation of LP events. The gases permeated the volcanic edifice, producing lubrication of pre-existing fractures and thus favoring the occurrence of VT earthquakes. On May 18, the flow front reached the shallow aquifer located under Las Cañadas caldera. The induced instability constituted the driving mechanism of the observed tremor.

Keywords: Teide volcano; Tenerife Island; volcanic earthquakes; volcanic tremor; seismic arrays; apparent slowness estimates

1. Introduction

The Teide–Pico Viejo–Cañadas volcanic system is probably one of the most important volcanic complexes

* Corresponding author. Tel.: +34 958 249552; fax: +34 958 160907.
E-mail address: alm@iag.ugr.es (J. Almendros).

0377-0273/$ - see front matter © 2006 Elsevier B.V. All rights reserved.
doi:10.1016/j.jvolgeores.2006.10.002

of Canary Islands. It is located in the center of Tenerife Island (Fig. 1), and constitutes the highest elevation (Teide, 3718 m) of the region. In the last 300 years, six effusive processes have been reported, being the last eruption that of Chinyero in 1909. There are evidences of explosive eruptions as well, for example the sub-plinean eruption occurred around 2000 years ago in Montaña Blanca, in the SE flank of Teide (Ablay et al., 1995). The presence of densely populated areas around the volcano edifice places this area among the most vulnerable regions in the Canary Islands archipelago.

Many studies have been carried out at Tenerife to investigate the volcanic structure and dynamics. We can mention gravimetric and geodetic surveys (Sevilla and Romero, 1991; Watts, 1994; Ablay and Kearey, 2000; Araña et al., 2000; Yu et al., 2000; Fernández et al., 2003); geochemical analyses (Hernández et al., 2000, 2004); magnetotelluric (Ortiz et al., 1986; Pous et al., 2002) and magnetic (Blanco, 1997; Araña et al., 2000) surveys; and regional and local seismicity studies (Mezcua et al., 1992; Del Pezzo et al., 1997; Canas et al., 1998; Canales et al., 2000; Almendros et al., 2000, 2004). All these works document the absence of evidences pointing to a reactivation of the volcanic system. However, in 2004 an unusual increment of seismic activity was detected by the IGN (Instituto Geográfico Nacional, Spain's National Geographic Institute) seismic network monitoring Tenerife Island. In Fig. 1b we show the recent seismicity around Tenerife, as reported in the IGN catalog (http://www.ign.es). Before 2004, epicenters clustered in an offshore area southeast of Tenerife. These earthquakes have been interpreted as a consequence of regional tectonic stresses (Mezcua et al., 1992; Canas et al., 1998). Very few earthquakes occurred in other areas, including Teide volcano. Starting in April 2004, there was a significant increase of the number of earthquakes in the vicinity of Teide (Fig. 1b,c). Some earthquakes were large enough ($M>3$) to be felt by population in nearby villages. As a consequence of this activity, the first steps of the emergency plans were activated, including meetings of a scientific committee, and civil protection consultations. The level of seismicity in the area stayed high up to September 2004. During the remaining of 2004 and the first half of 2005, the activity decreased (M. J. Blanco, personal communication).

In May 2004, as a response to the increment of seismicity detected, a temporary survey involving three seismic antennas was carried out at Las Cañadas caldera. In this paper, we present the analysis of seismic data obtained from this survey. We report not only the occurrence of earthquakes related to Teide volcano, but also the appearance of fluid-related seismicity, including volcanic tremor. We interpret these signals as the

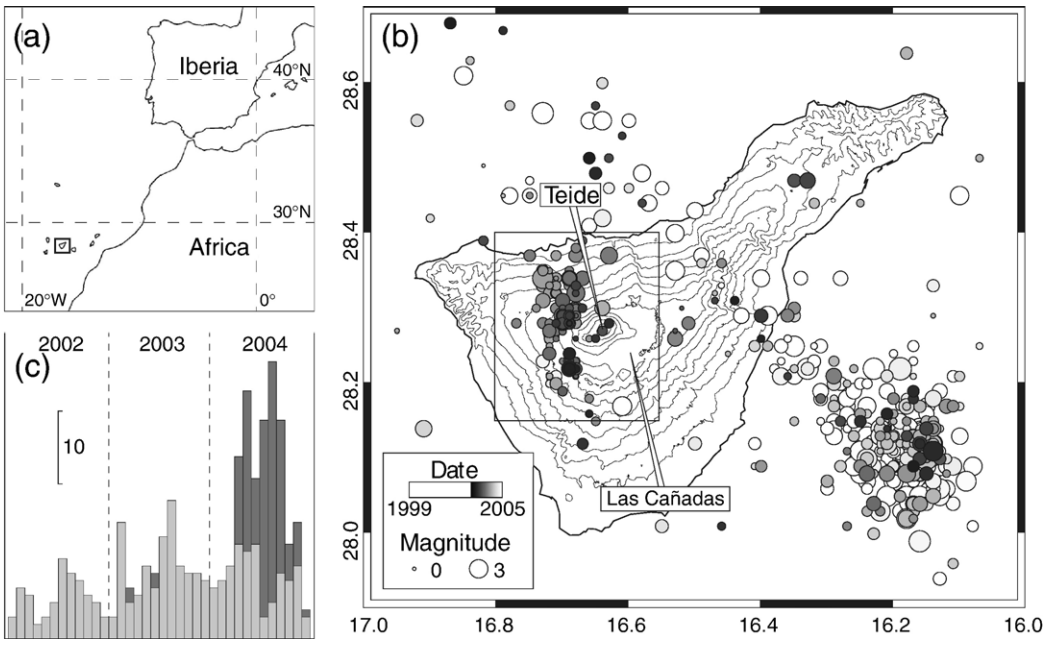

Fig. 1. (a) Location of Canary Islands archipelago in the northwest margin of the African plate. (b) Map of Tenerife Island, showing the epicenters provided by IGN for the period 1999–2005. Colors and sizes of the dots are related to the earthquake origin times and magnitudes, respectively. The box around Teide volcano marks the epicentral area of the 2004 seismic swarm. (c) Histogram of the number of earthquakes per month during the period 2002–2004. Light and dark gray respectively represent earthquakes occurring outside and inside the Teide volcano region (the box in (b)).

response of the medium to a magmatic injection in depth.

2. Instruments and data

We deployed three seismic antennas at Las Cañadas caldera in early May 2004. We selected three locations near Teide volcano: Cañada de Diego Hernández (DH), Sanatorio Plateau (SA) and the southern slopes of Pico Viejo volcano (PV) (see Fig. 2). Each antenna was composed of 10 short-period seismometers (nine vertical-component and one three-component). All receivers were Mark L28 instruments, with response electronically extended to 1 Hz. The acquisition system sampled these 12 channels at 100 sps with a 24-bit A/D converter in continuous mode. Data was stored into an external, 30 Gb hard disk. Absolute timing was obtained using a GPS receiver. The DH, SA, and PV antennas had apertures of 550, 430, and 350 m, respectively. They were in operation during the period May–July 2004. Unfortunately, due to the difficulties of maintenance, the antennas worked only intermittently during the last period of the survey. In this work, we selected for the analysis the initial (and most active) period of the survey (Fig. 3).

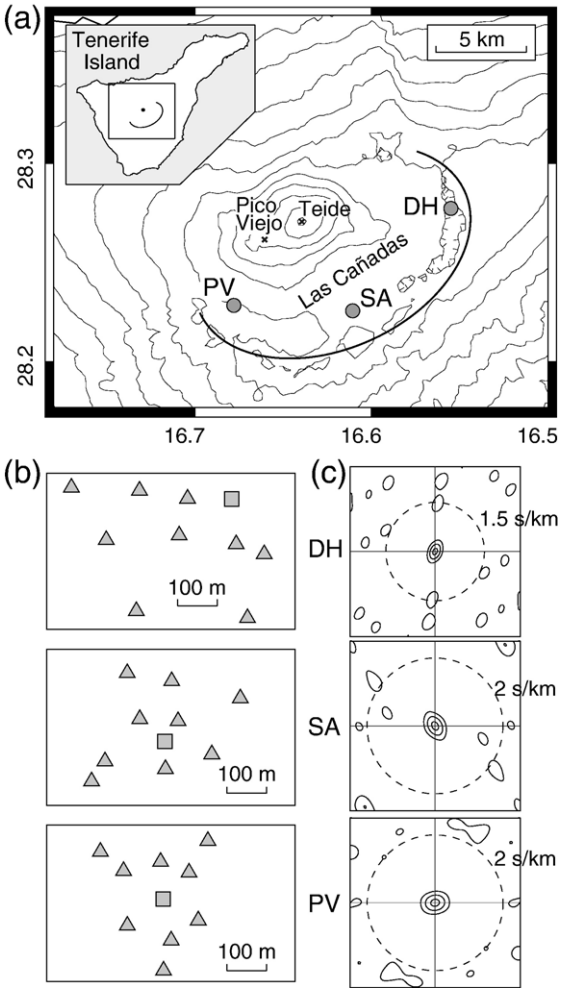

Fig. 2. (a) Locations of the seismic antennas used in this study at three sites within Las Cañadas caldera in central Tenerife: Diego Hernández (DH), Sanatorio (SA) and Pico Viejo (PV). The thick line shows the approximate position of the caldera wall. (b) Configurations of the seismic antennas. Triangles correspond to vertical-component seismometers, while squares mark the positions of three-component sensors. (c) Beam forming array response calculated at 4 Hz for each antenna, contoured at 30, 60, and 90%. The dashed circles indicate the approximate distances to the closest secondary peaks produced by spatial aliasing.

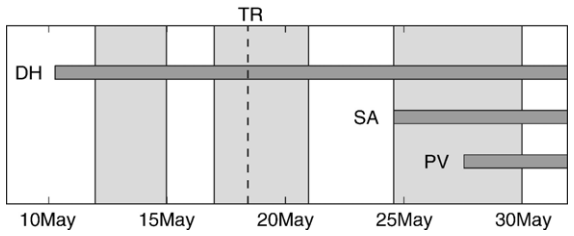

Fig. 3. Sketch of the time periods when the seismic antennas were operative at Las Cañadas caldera. The vertical bands show three periods selected for the analysis of continuous signals. The dashed line labeled 'TR' marks the start of the tremor signal (see text for explanations).

An inspection of the continuous record shows the presence of several signals with different characteristics. The most persistent is a low-frequency signal with frequencies below 1 Hz (Fig. 4a), that has been associated with microseismic noise of oceanic origin (Almendros et al., 2000). Superimposed to this background signal, our data contains several hundreds of small volcano-tectonic (VT) earthquakes, characterized by short durations, high-frequency contents, and wide spectra (Fig. 4b). A few long-period (LP) events, generally associated with the presence of volcanic or hydrothermal fluids (e.g. Chouet, 1996), have been also recorded (Fig. 4c). For these events, most of the energy is concentrated in the 2–5 Hz frequency band. Nevertheless, the most striking feature of the seismic wavefield at Las Cañadas caldera was the appearance of a continuous tremor characterized by a narrow-band spectral content at variable frequencies between 1 and 6 Hz (Fig. 4d).

The appearance of volcanic tremor is a unique observation at Teide volcano. Such kind of seismic signal has never been detected in previous surveys, including those performed by our group (with the same instruments and in the same areas) in 1994, 2000–2001,

and 2003–2004. The only continuous, ubiquitous signals formerly reported were the oceanic microseisms (Almendros et al., 2000), recorded at ~1 Hz in our short-period instruments (Fig. 4). However, at about 10:00 UTC on May 18, 2004, a second continuous, quasi-monochromatic signal emerged from this low-frequency oceanic noise (see Fig. 5). Its central frequency slowly increased with time, and stabilized some six hours later at about 4–5 Hz, with occasional variations later on. The spectrogram reveals small oscillations of the tremor frequency, with peak-to-peak amplitudes smaller than 0.5 Hz and periods of several tens of seconds. Its amplitude was low, and showed frequent modulations (Fig. 4d). Takagi et al. (2006) describe the occurrence of volcanic tremor with similar waveform characteristics at Aso volcano, Japan, although they do not report any temporal variations of the spectral content. The tremor recorded at Teide volcano lasted for at least several weeks, beyond the period analyzed in this work. The tremor onset was recorded only at the DH antenna, since the others began to function after May 18 (Fig. 3). During the last part of May, all our instruments operated simultaneously. We recorded similar signals at all three antenna locations (Fig. 6), which excludes the presence of noticeable path effects.

As a final remark, note that the faint bands in Figs. 4–6, for example at 5 and 10 Hz for the DH antenna, are but incoherent, unfiltered electronic noise generated by the acquisition systems.

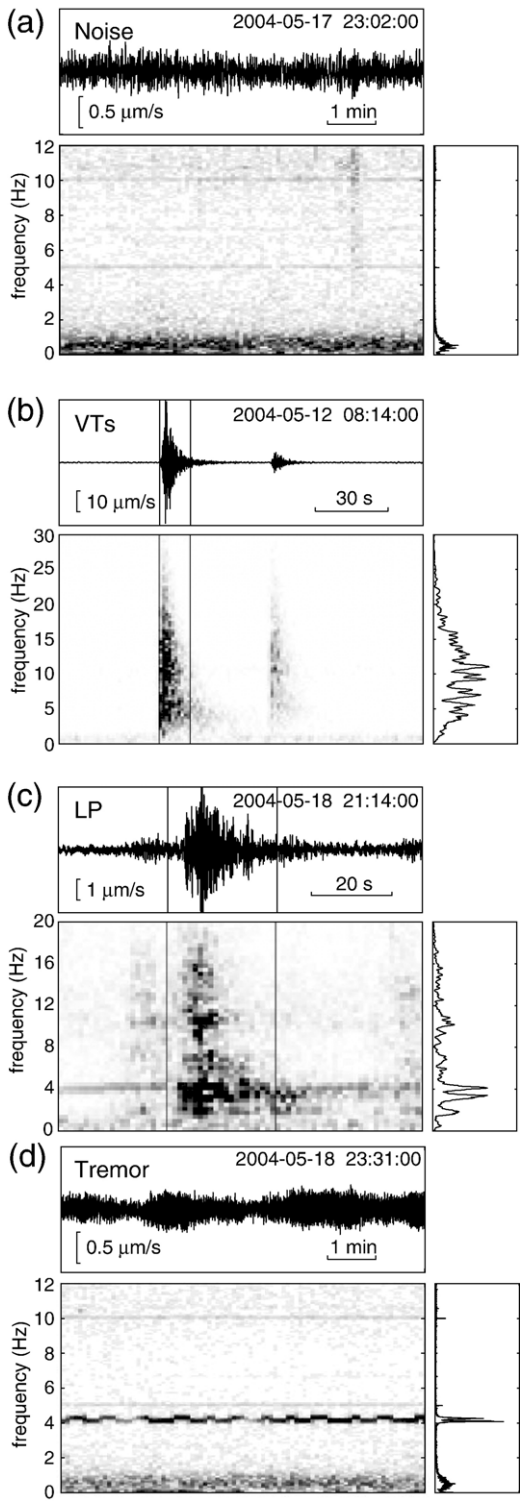

Fig. 4. Vertical-component seismograms, spectrograms, and spectra of different types of seismic signals: (a) microtremor noise, (b) volcano-tectonic earthquakes, (c) long-period event, and (d) continuous tremor. Spectra in (b) and (c) correspond to the piece of data between the vertical lines in the seismograms and spectrograms. In (a) and (d), the whole time windows displayed were used to compute the spectra.

3. Method and results

We applied the zero-lag cross-correlation (ZLCC) method (Frankel, 1994; Del Pezzo et al., 1997; Almendros et al., 1999) to array data in the period May 12–31, 2004, in order to estimate the apparent slownesses and propagation azimuths of the recorded wavefields. Based on the spectral characteristics of the seismic data described above, we selected three frequency bands for the analysis: 0.5–2 Hz for oceanic microseisms; 2–8 Hz for LP events and tremor; and 8–15 Hz for VT earthquakes. We used window lengths of 1.5, 0.5, and 0.4 s, respectively. Successive time windows overlapped 50% of the window length. Taking into account the array configurations, we selected a common slowness vector grid between −3 and 3 s/km both in east–west and north–south directions, with a

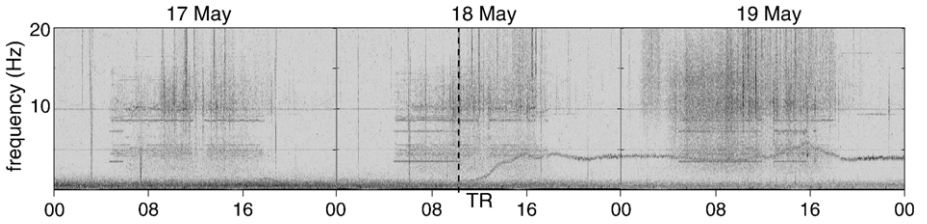

Fig. 5. Vertical-component spectrogram of three days of seismic data (from May 17 to 19) at the DH antenna. The plot was obtained with a FFT window length of 10.24 s. The dashed line marks the initial stages of tremor at about 10:00 on May 18.

grid spacing of 0.05 s/km, for all the analyses. However, and in order to avoid the effects of spatial aliasing, we restricted our results to apparent slowness values below 2 s/km for the SA and PV antennas, and below 1.5 s/km for the sparser DH antenna. For transient events (VT earthquakes and LP events), we applied the ZLCC method to 20 s of data centered at the first arrival. For continuous signals (oceanic noise and tremor), we applied the ZLCC method to the three periods indicated in Fig. 3.

3.1. Oceanic microseisms

The low-frequency band between 0.5 and 2 Hz contains basically the high-frequency shoulder of the oceanic noise spectrum, generally peaked at periods of several seconds (e.g. Aki and Richards, 2002, p. 617). Fig. 7 shows an example of the results obtained for one hour of data at the PV antenna. In this band, the wavefields are always characterized by high correlations among the array stations, high apparent velocities, and absence of preferred back-azimuth directions. These propagation properties remain unchanged over the whole analyzed period, and coincide with those observed in a previous study (Almendros et al., 2000).

3.2. VT earthquakes and LP events

The identification of the VT earthquakes was performed visually on the continuous records, using the three-component station of the DH array. We selected this antenna because it was the first to start operations; it worked for a period longer than the other two antennas; and finally, the selection of this site allow us to compare our results with those from a couple of previous seismic surveys that were carried out in the Cañada de Diego Hernández as well (Del Pezzo et al., 1997; Almendros et al., 2000). We determined P- and S-wave arrival times for about 220 VT earthquakes recorded during the period May 12–31. To obtain the propagation parameters of the P-wave arrival of the selected earthquakes, we applied the ZLCC method using the 8–15 Hz frequency band, where the signal-to-noise ratio was highest. The background noise at this frequency has an average correlation of 0.2. Therefore, we selected those array solutions with correlations greater than 0.5 (2.5 times the noise correlation). In this way, we obtained robust estimates of apparent slownesses and back-azimuths for 97 VT earthquakes. In order to use this information to derive hypocenter positions, we need a velocity model for the medium. However, there are no specific models developed yet for Las Cañadas caldera or Teide volcano. We followed Almendros et al. (2000) and used a model derived for Etna Volcano. The source locations were calculated by ray-tracing through this model, using the S–P times to fix the distances. The results are shown in Fig. 8. Although VT source locations might be severely biased due to the lack of an adequate velocity model, we are still able to track the relative changes in source

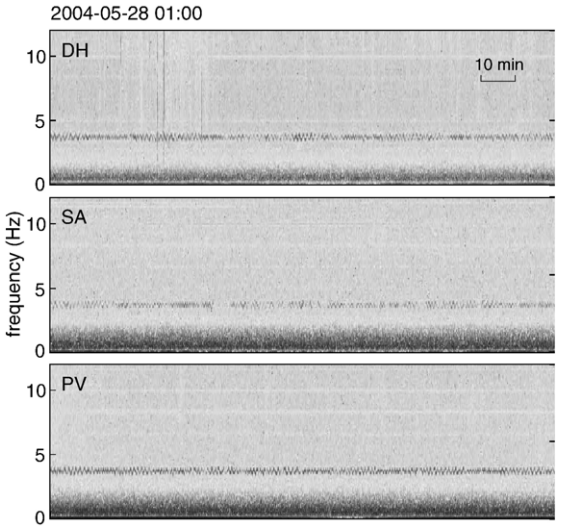

Fig. 6. Vertical-component spectrograms of the tremor signal at antennas DH (top), SA (middle) and PV (bottom). The plot starts at 01:00 on May 28, and represents 2.5 h of data. The FFT window length is 10.24 s.

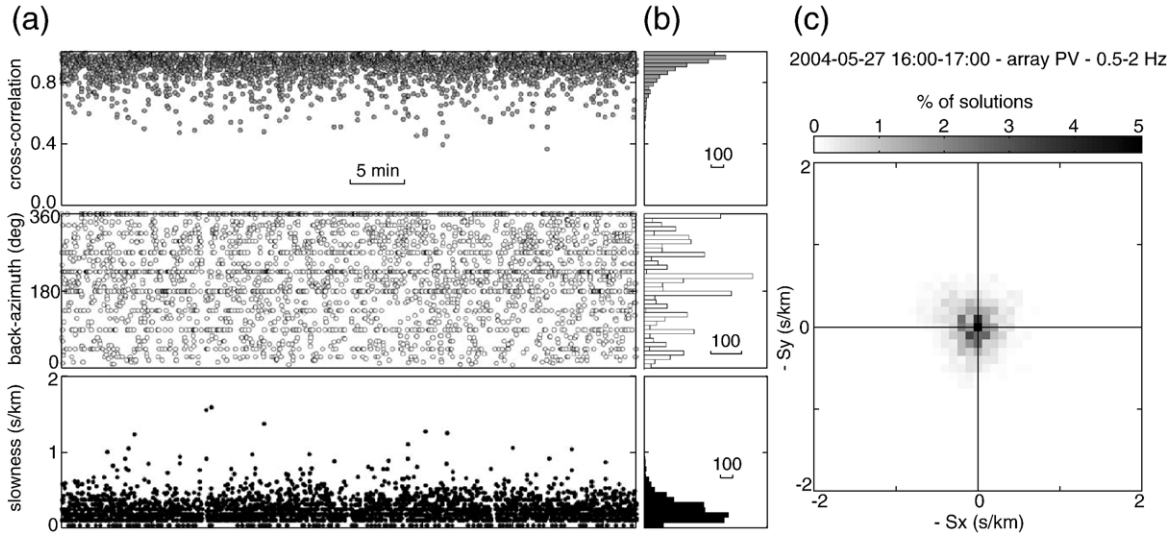

Fig. 7. Example of the results of the cross-correlation technique in the 0.5–2.0 Hz band. (a) One hour of array solutions plotted versus time. From top to bottom, we display maximum array-averaged cross-correlation, back-azimuth, and apparent slowness. (b) Histograms of the array solutions shown in (a). (c) 2D histogram of the array solutions in the slowness vectors domain. Slowness vector components are reversed in sign to indicate back-azimuth.

locations. In this sense, we observe two distinct patterns in the spatial distribution of VT earthquakes. Early earthquake locations cluster below the northwest flank of Teide volcano, at large depths (>14 km). In the second half of May, the pattern seems to change, showing a larger dispersion both in epicentral position and depth. VT earthquakes spread beneath Las Cañadas caldera, far from the initial cluster. They occur at a wide

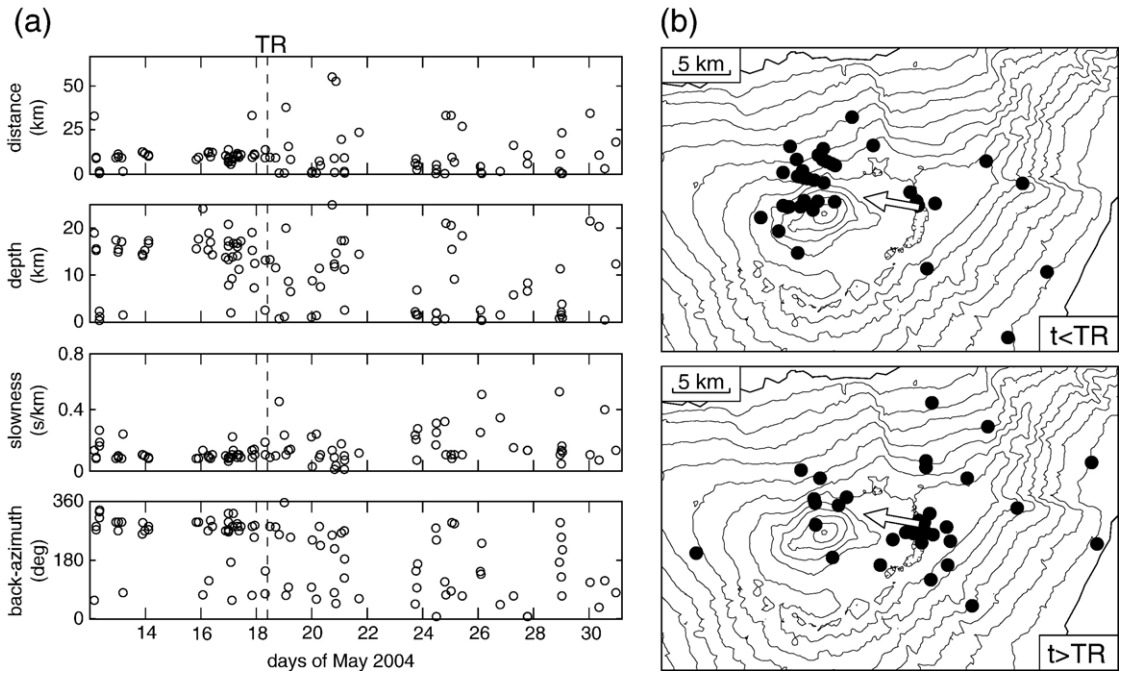

Fig. 8. (a) Temporal distribution of distance, depth, apparent slowness and back-azimuth estimated for the VT earthquakes recorded during May 2004. The dashed line labeled "TR" marks the start of the tremor signal on May 18. (b) Epicenters of VT earthquakes that occurred before (top) and after (bottom) the start of tremor. The white arrow indicates the average back-azimuth corresponding to the analyzed LP events.

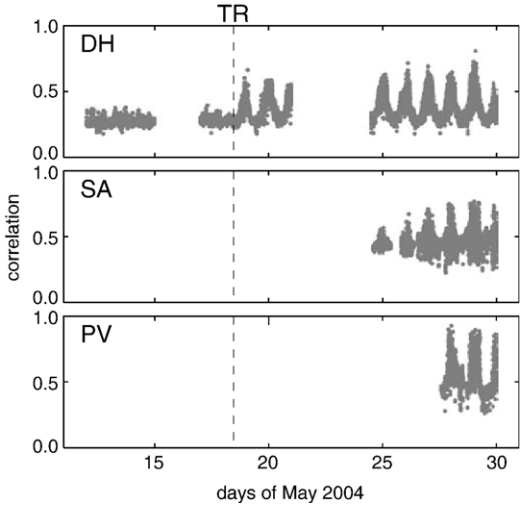

Fig. 9. Maximum array-averaged cross-correlation versus time at the three antennas for the periods selected for the analysis (see Fig. 3).

depth range; in fact, more than 40% of the earthquakes are shallower than 3 km.

From visual and spectral inspection of the DH continuous record, we identified 5 events that can be regarded as LP events (Fig. 4c). We selected the 2–8 Hz band for the ZLCC analysis. The average noise correlation at this frequency band is about 0.3, while the maximum correlations of the LP events are around 0.9. Back-azimuths and apparent slownesses coincide with those corresponding to the VT cluster occurring northwest of Teide. In Fig. 8b we plotted an arrow showing the average back-azimuth of the LP events. LP and VT apparent slowness values are also similar, about 0.15 s/km. Assuming that the first onsets of the LP events are P waves, we hypothesize that LP events and VT earthquakes share a common source volume, a deep region northwest of the Teide summit.

3.3. Continuous tremor

We performed ZLCC analyses of the tremor records in the 2–8 Hz band for the three periods displayed in Fig. 3. The extremely low amplitude constitutes a challenge for the capabilities of the seismic antennas. Fig. 9 shows the maximum array-averaged cross-correlation obtained during the analyzed periods. Before the tremor begins, the correlation is consistently low, with average values around 0.3. No coherent seismic sources were present in the wavefield. In particular, this demonstrates that the electronic noise generated by the acquisition system has virtually no effect in the ZLCC array results. After the tremor starts, we detect a general increase of the cross-correlation, with peak values up to 0.7. The correlation displays an oscillatory behavior with a period of 24 h, related to the day/night cycle. The correlation highs and lows coincide with nighttimes and daytimes, respectively. We infer that the seismic antennas have more trouble identifying the weak tremor signal during the day than during the night, due to the different levels of cultural noise (see Fig. 5). The most accurate results happen in nocturnal periods, when the sources of cultural noise have died off. Figs. 10 and 11

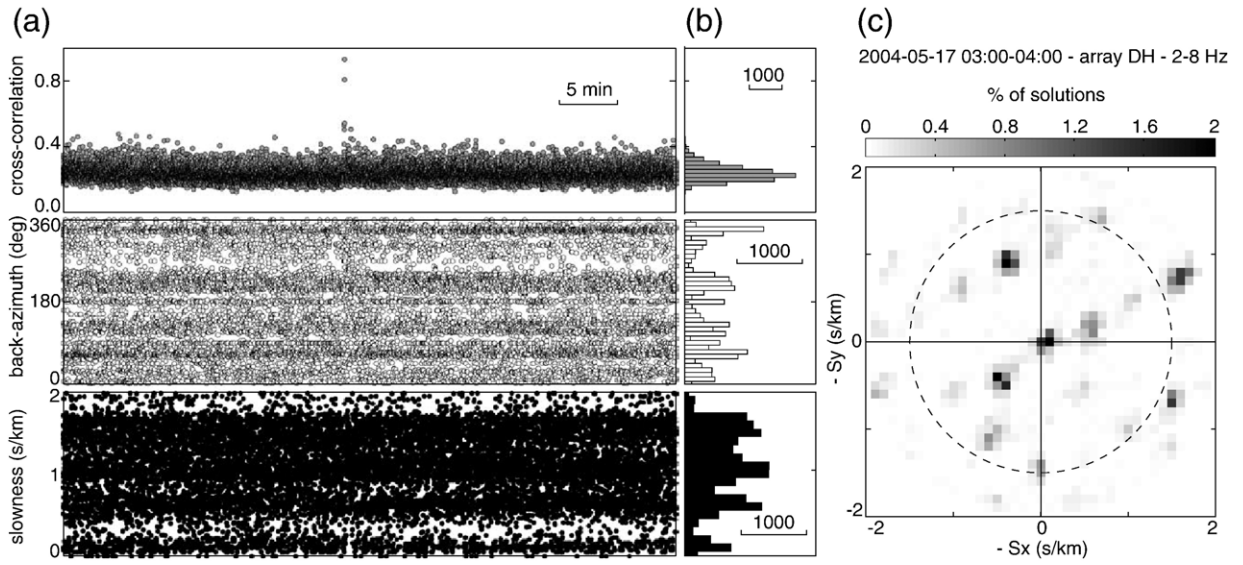

Fig. 10. Results of the ZLCC technique in the 2–8 Hz band for one hour of data before the start of tremor on May 18, 2004. See Fig. 7 for explanations.

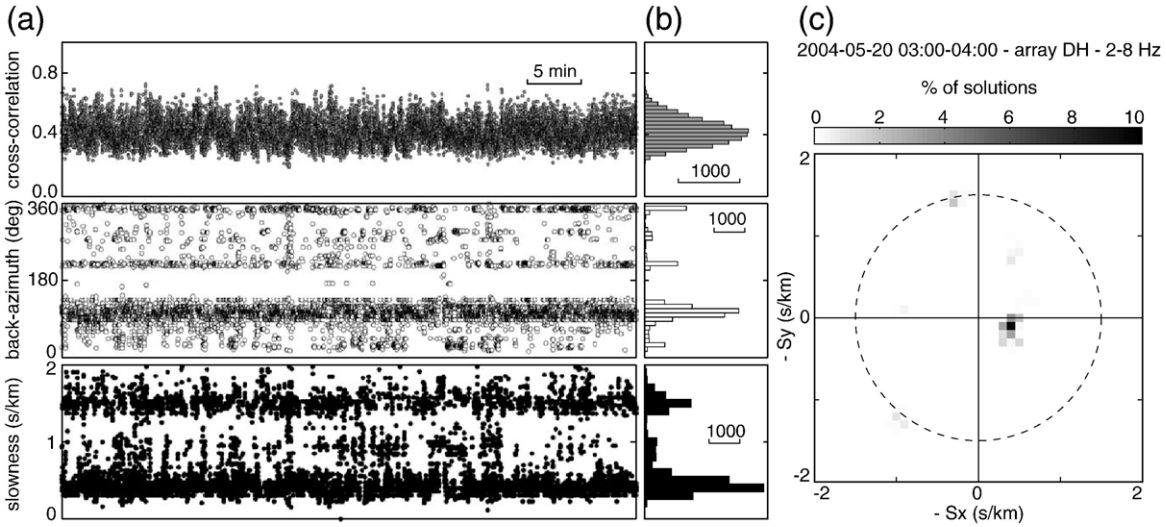

Fig. 11. Results of the ZLCC technique in the 2–8 Hz band for one hour of data after the start of tremor on May 18, 2004. See Fig. 7 for explanations.

show the results of array analyses for two hours of data recorded before and after the start of tremor, respectively. These plots evidence the different characteristics of the wavefields. Fig. 10 corresponds to data recorded a few hours before the tremor onset. It reveals a wavefield composed of incoherent wave arrivals. The values of correlation are low, and there are large dispersions in the apparent slownesses and back-azimuths. Conversely, Fig. 11 corresponds to data recorded after the tremor onset. It shows higher values of correlation and stable, well-defined apparent slowness and back-azimuth solutions.

The characteristics of the wavefield evolve during the time period analyzed. We observe changes of apparent slowness and/or back-azimuth of the dominant component of the wave-field, as well as the simultaneous presence of wavefield components characterized by different slowness vectors. Accordingly, we infer the existence of multiple seismic sources in the wave-field, acting either successively or simultaneously. Fig. 12 shows hourly histograms of the apparent slowness vectors estimated at the DH antenna. Compared with Fig. 11, the dominant back-azimuths are clearly different, indicating the activation of new seismic sources. Moreover, the three panels of Fig. 12 show two peaks in similar positions, suggesting the presence of two sources at back-azimuths of 40–50 and 240–250°N, respectively. The relative heights of these peaks indicate which source dominates at that particular time. A third peak in the SW quadrant of the central panel has been dismissed. Its apparent slowness is larger than the limit of 1.5 s/km imposed for the DH antenna to avoid the erroneous interpretation of aliased peaks.

Unfortunately, the comparison of the results provided by the three antennas deployed in Las Cañadas caldera reveals that their descriptions of the wavefield are barely compatible. Variations in apparent slowness and back-azimuth do not generally correlate at different antennas. Moreover, simultaneous estimates of apparent slowness vectors are not consistent with the presence of single sources, thus preventing the determination of the source position using a joint location method (Almendros et al., 2000, 2001; Métaxian et al., 2002; Saccorotti et al., 2004). Fig. 13 constitutes a rough, unsuccessful attempt at source location. It shows apparent slowness and back-azimuth results for 10 s of data recorded at the three seismic antennas. The high correlations and stable solutions indicate the presence of coherent, continuous seismic sources. The back-azimuths point consistently to the NE, SE, and SSE for the DH, SA, and PV antennas, respectively. Obviously, this geometry is not compatible with a single source, and consequently a joint location cannot be accomplished. This result suggests the existence of multiple, low-energy tremor sources acting simultaneously. The antennas would focus on the nearest sources, being unable to extract any useful information for the more distant sources.

Due to the inconsistency of the slowness vectors solutions among the arrays, a quantitative joint location cannot be determined. However, the interpretation of the dominant slowness vectors might yield qualitative information about the source characteristics and locations (e.g. Almendros et al., 2002). Fig. 14 shows the dominant apparent slowness vectors identified with the ZLCC analyses between May 27 and 30. In this period, the three antennas operated simultaneously, and therefore a joint interpretation of the slowness vectors could be possible.

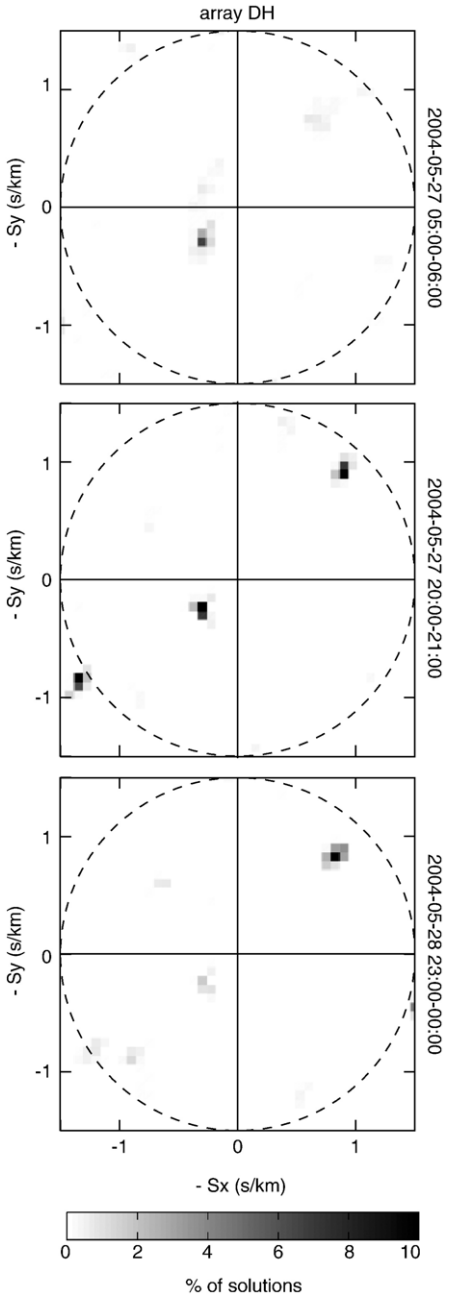

Fig. 12. Examples of hourly histograms of apparent slowness in the 2–8 Hz band for the DH array. The dashed circle represents the maximum apparent slowness allowed for the antenna. Slowness vectors components have been reversed in sign to indicate back-azimuths.

However, the observed vectors do not usually fit within simple explanations. For example, some slowness vectors diverge from the Las Cañadas caldera (i.e. DH 1, SA 1, PV 1 and 2). They could be related to shallow sources along the caldera wall. The slowness vector estimates performed at the DH antenna immediately after the start of tremor (the white arrow in Fig. 14) could be also related to a source in the caldera wall. The small apparent slowness suggests a slightly deeper source. Slowness vectors SA 2 and PV 3 could correspond to a single signal propagating from a back-azimuth of about 300°N. The parallel directions suggest a distant source. This interpretation leaves slowness vector DH 2 unexplained. Even considering the relatively large azimuthal deviations expected at volcanic areas, due to the effects of topography and other lateral heterogeneities (Almendros et al., 2001; Métaxian et al., 2006), it is hard to relate DH 2 to the same source identified by SA 2 and PV 3. Moreover, since it points toward the center of the caldera, it is highly unlikely that the SA antenna would not detect a signal with northeast back-azimuth. An alternative explanation would be that slowness vectors DH 2 and SA 2 represent a common source. Their back-azimuths point to an area south of Teide volcano, near the SA antenna. The apparent slowness is larger for the SA array, located closer to the source, as expected. In this case, slowness vector PV 3 would correspond to a source located somewhere in the western border of the caldera.

4. Discussion

We have analyzed three weeks of continuous data recorded by three seismic antennas deployed at Las Cañadas caldera. These data belong to one of the most intense seismic episodes recently reported in the area. The activity began in April 2004 with the occurrence of several earthquakes under the northwest flank of Teide volcano, as reported by IGN. Some of them reached magnitudes larger than 3, and were felt at nearby villages. We estimated source locations for 92 earthquakes recorded between May 12 and May 31. During the first days of this period, VT earthquakes clustered beneath the northwest flank of Teide at depths larger than 14 km. Within the limitations of our location procedure, these earthquakes do not seem to be aligned along any preferential direction. The depth of the source volume is compatible with the inferred depth of the basaltic magma chamber (Martí et al., 1994; Ablay and Martí, 2000; Araña et al., 2000; Martí and Gudmundsson, 2000). Taken together, these observations suggest that the early stage of VT activity was likely driven by forces associated with a magmatic reactivation rather than by regional tectonic stresses acting on well-defined rupture planes. We have identified a few LP events whose source locations probably coincide with the position of the VT cluster. Although most LP events recorded at volcanic areas around the world are shallow (Chouet et al., 1994; Gil Cruz and Chouet, 1997; Ibáñez et al., 2000; Almendros et al., 2001; Arciniega Ceballos et al., 2003; Caliro et al.,

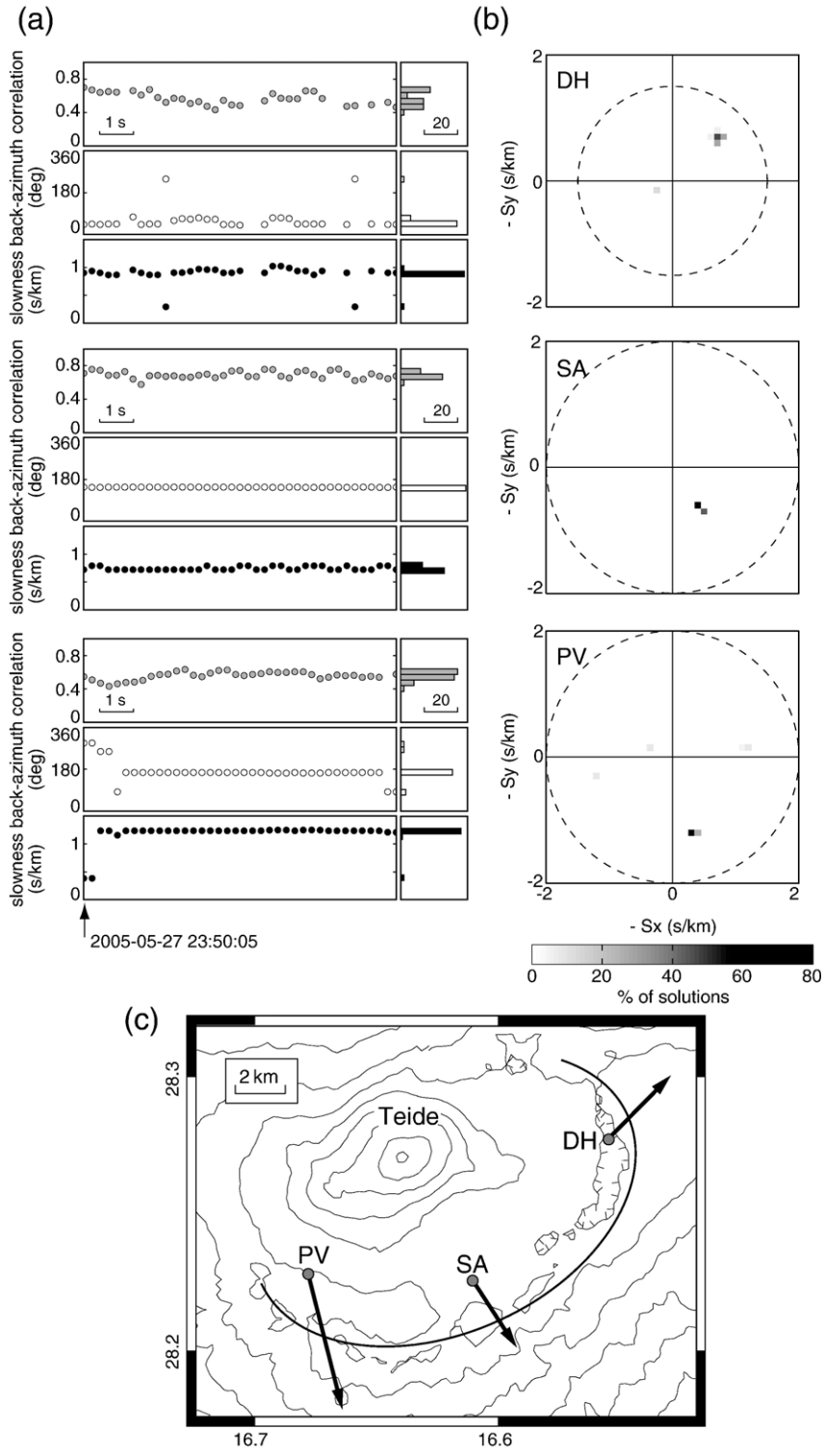

Fig. 13. Results of the ZLCC analyses at the three antennas for 10 s of data recorded during the night of May 27. (a) Time series and histograms of correlation, back-azimuth and apparent slowness. (b) 2D histograms of slowness vectors. The top, center, and bottom rows correspond to the DH, SA, and PV antennas, respectively. The dashed circle represents the maximum apparent slowness allowed for the antenna. (c) Map of the Las Cañadas caldera, showing the average apparent slowness vectors, estimated in the time window displayed in (a), at the corresponding seismic antenna locations. In (b) and (c), slowness vectors components have been reversed in sign to indicate back-azimuths.

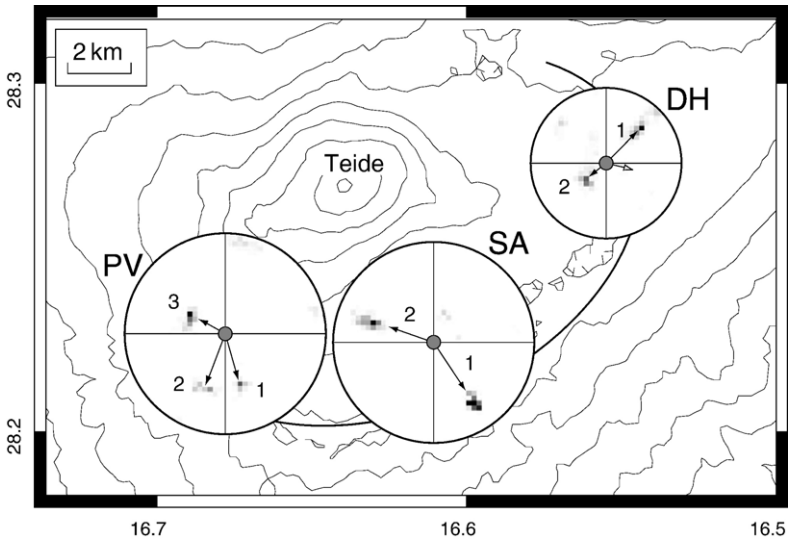

Fig. 14. Histograms of apparent slowness and back-azimuth results obtained from the analysis of tremor at the three antennas. The position of the antennas is marked by gray dots. The large circles represent slowness vector domains centered at the array location. They contain slowness vector histograms for the high-correlation solutions obtained between May 27 and 30, when the three seismic arrays operated simultaneously. The radius of the circles correspond to apparent slownesses of 1.5 s/km for the DH antenna, and 2 s/km for the SA and PV arrays. The arrows represent the slowness vectors that appeared persistently in the wavefields. Slowness vectors components have been reversed in sign to indicate back-azimuths.

2005), the occurrence of deep LP events is not rare (Battaglia et al., 2003; Power et al., 2004; Ukawa, 2005; Soosalu et al., 2006). The presence of LP events within the VT source volume reveals the presence of volcanic fluids, and supports the hypothesis of a volcanic origin for the VT earthquake cluster. During the second half of May 2004, the deep VT cluster became less active. Estimated source locations spread all over Las Cañadas caldera, at depths ranging up to the surface. On May 18 we detected the occurrence of volcanic tremor, lasting for at least several weeks. This tremor was recorded in the whole caldera by three antennas separated up to 20 km, regardless of its low amplitude. Array solutions suggest the simultaneous presence of multiple tremor sources. The antennas catch glimpses of several sources that remain active for a while, being the array solutions related to the most energetic sources (or nearest to the array) in that particular time.

We propose the following model to explain the seismic activity produced during April–May 2004 at Teide volcano. In early April, an injection of basaltic magma took place at depths below 14 km. This injection generated a change in the stress distribution around the magmatic chamber, and triggered the occurrence of VT earthquakes (Fig. 15a). In turn, the occurrence of seismicity allowed for an enhanced rate of magma degassing. At an initial stage, the upward-migrating volatiles induced the resonance of deep fluid-filled cavities, thus producing the deep LP activity (Fig. 15a). During the following days, the gas flow front propagated upward by diffusion through the medium. This fluid migration may produce lubrication of fractures. Fluid overpressure lowers the friction coefficient and reduces the normal stress, favoring the occurrence of brittle fracture earthquakes without increasing the seismic stress field (e.g. Brodsky and Kanamori, 2001). Since the volcanic edifice is highly fractured, especially in the shallow layers, the gas flow may induce brittle fractures in pre-existing cracks (Fig. 15b). The consequence would be the spread distribution of VT earthquakes observed in the second half of May 2004. Finally, when the gas reached the surface, it could interact with the shallow aquifers and produce volcanic tremor.

This series of events explains the basic features observed in our data. Moreover, there are other evidences that support this model. First of all, the estimated source depths of the initial VT earthquake cluster may be compatible with the depth of the basaltic magma supply zone assumed beneath Las Cañadas caldera. Several studies have investigated the volcanic structure below Las Cañadas caldera using geological and geophysical data (e.g. Martí et al., 1994; Ablay and Martí, 2000; Araña et al., 2000). The inferred structure is characterized by shallow (~4–5 km), phonolitic magma chambers linked to the volcanic evolution of Las Cañadas edifice, and a deeper (~13–15 km) reservoir containing basaltic magma. This area probably constitutes the source of the recent basaltic eruptions occurred in Tenerife. The estimated VT source depths suggest that VT earthquakes could be connected to the deep magma supply zone.

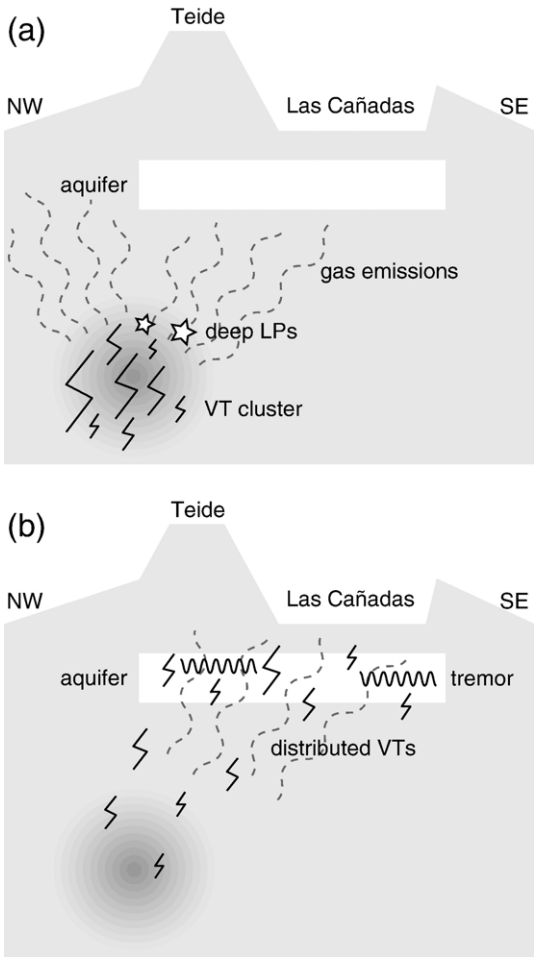

Fig. 15. Sketch of our interpretation of the seismic events that occurred during May 2004. (a) Situation before May 18. A deep magma injection occurs beneath Teide volcano. It produces a VT swarm and an enhanced gas emission stimulating the occurrence of LP events. (b) Situation after May 18. The fluid pressure lubricates pre-existing faults, inducing VT earthquakes throughout the medium. The gas flow front interacts with the shallow aquifer and generates continuous tremor.

However, we cannot rule out completely a link with the shallow magma chambers, due to the large depth uncertainties in the location procedure. A second piece of evidence comes from gas measurements. Although the amount of gas emitted in Tenerife is small compared to other active volcanoes, gas emissions in Las Cañadas caldera are important and have been studied in detail (Pérez et al., 1996; Hernández et al., 2000, 2004). Part of the supply of gas is probably due to volcanic activity (Galindo et al., 2005). A deep aquifer located at about sea level acts as a filter, cooling the gas and withdrawing many of its soluble components. In such a system, a magma injection in depth would be followed by an increase of the emission of volcanic gases through the surface. In fact, an increase of the diffuse CO_2 emissions related to the 2004 activity has been described by Pérez et al. (2005) shortly after the start of the seismic crisis. They detected an excess of CO_2 in the flanks of Teide volcano, representing several times the baseline measured during the previous years.

According to the model presented above, the injection process most likely started in early April, when the VT activity began to increase. The onset of volcanic tremor on May 18 indicates the arrival of the gas pressure front to the surface. Thus, magmatic gases required 40–50 days to propagate through the medium up to the free surface. Assuming that the injection occurred at a depth of about 15 km, the average velocity of the gas propagation toward the surface is ~300 m/day. The average diffusivity of the medium, D, can be estimated using the relation $r = \sqrt{4\pi Dt}$ proposed by Shapiro et al. (1997), where r is the distance traveled by the flow front at time t. The diffusivity of crustal rocks ranges between 0.01 and 10 m^2/s (Talwani and Acree, 1984; Ferreira et al., 1995; Shapiro et al., 1999; Talwani et al., 1999), although larger values have also been measured (Noir et al., 1997; Shapiro et al., 2003; Antonioli et al., 2005). Saccorotti et al. (2002) analyzed a seismic swarm related to diffusive processes at Vesuvius volcano, and derived a value of $D \sim 0.2$ m^2/s. Our calculations yield a diffusivity of 4–5 m^2/s, well within the above ranges, which supports our hypothesis of a magmatic injection episode at Teide volcano.

The origin of the volcanic tremor recorded at Las Cañadas caldera is a very interesting and intriguing question. Several mechanisms have been proposed to explain the generation of tremor in volcanic and geothermal environments. For example we can cite resonance of fluid-filled conduits with different geometries (Chouet, 1985, 1986; Fujita et al., 1995; Fukao et al., 1998; Fujita and Ida, 2003), fluid flow effects (Julian, 1994; Hellweg, 2000), bubble collapse (Kedar et al., 1998), and two-phase fluid flow instabilities (Iwamura and Kaneshima, 2005). It is likely that the primary process driving the tremor sources is related to interactions between a shallow aquifer and an increased supply of magmatic gases liberated by the deep magma injection. There is a shallow aquifer forming independent pools under Las Cañadas caldera, with different water table depths between 300 and 450 m below the surface. Geochemical monitoring of these waters indicate a water temperature about 16 °C and saturation in CO_2 (Hernández et al., 2000; Soler et al., 2004). Further supply of CO_2 would produce a net decrease of fluid density and an increase of the impedance contrast with the surrounding rocks, favoring the trapping of

seismic energy and the resonance mechanisms. Moreover, the massive gas supply from below would induce sudden pressure steps and turbulent flows throughout the fracture network pertaining to the aquifer, providing the triggers for the resonance processes. Volcanic gases probably circulated through the weakest (hence most permeable) zones, such as hydrothermally-altered areas and the caldera wall (Galindo et al., 2005). This flow could induce the simultaneous activation of different parts of the crack system, which is consistent with the presence of multiple, apparently unrelated sources in the tremor wavefield (Fig. 14). However, the long duration, high stability, and spatial homogeneity of the tremor signal challenge this interpretation. Tremor models assume that the tremor frequency is related to the physical properties of the fluid and the characteristics of the surrounding solid medium. Since tremor spectra at the three array sites are very similar (Fig. 6), we should conclude that several sources of the same size and shape and related to precisely the same mixture of CO_2 and water act simultaneously at different locations. However, this is a rather unlikely occurrence. Instead, we expect that the volcanic gases interact with an irregular, heterogeneous system of cracks and conduits within the aquifer. Moreover, the gas–water mixture could have different compositions, depending among other factors on the amount and composition of the gas supplied.

The slow shifting of the central frequency of the tremor signal (see for example Fig. 5) could imply an evolution of the tremor source. For example, between 10:00 and 16:00 on May 18 the tremor frequency varies from 1 Hz to about 6 Hz. Similar long-term fluctuations of tremor frequency at different time scales have been reported at several volcanoes, for example Villarrica, Chile (Ortiz et al., 2003), Arenal, Costa Rica (Lesage et al., 2006), and Soufriere Hills, Montserrat (Powell and Neuberg, 2003). These variations could be interpreted in several ways. For example, changes in the tremor frequency would be expected when there are changes in the sizes of the resonating cavities or conduits. A more feasible explanation is that the shift of frequency may reflect a change in the fluid properties (e.g. Benoit and McNutt, 1997; Kumagai et al., 2002). In our model, the tremor begins when the gas starts flowing through the aquifer. The gas flow could induce bubble growth and increase the gas volume fraction in the CO_2–water mixture. However, the effect of an increase of gas content in bubbly liquids is a small reduction of the acoustic velocity (Kumagai and Chouet, 2000), which is not consistent with the observed increase of frequency. An alternative explanation suggests that tremor is originated by the repeated occurrence of single events at rapid, regular intervals (Hagerty et al., 2000; Neuberg et al., 2000). Variations of the tremor frequency would be related to changes in the triggering frequency of these events. In any case, the appropriate interpretation of the frequency variations of volcanic tremor observed at Teide is an open question that could be addressed in future works.

In our opinion, the 2004 unrest process at Teide volcano is a consequence of a deep magma injection that did not end in a volcanic eruption. The fundamental external observable that revealed the internal activity was the increase of seismicity. In Tenerife, there are indeed historical records that reveal the occurrence of felt seismicity before an eruption. Realtime monitoring using seismic networks and antennas will allow for the detection and interpretation of the different types of volcano seismicity in terms of internal phenomena.

Acknowledgments

We are grateful to G. Saccorotti, E. Fujita, and M. Mangan for their useful comments and suggestions. We thank IGN, the IGN team at Tenerife, and specially M. J. Blanco for useful discussions and support. We also thank J. Doniz, C. Romero, and all participants in the field experiment at Las Cañadas. This work was partially supported by the Spanish Ministry of Education, under Grants AMB99-1015-C02-02, CGL2004-05744-C04-01, and CGL2004-2001-E; by the European Union project VOLUME (FP6-2004-Global-3-018471); and by the research team RNM-104 of Junta de Andalucía, Spain.

References

Ablay, G.J., Kearey, P., 2000. Gravity constraints on the structure and volcanic evolution of Tenerife, Canary Islands. J. Geophys. Res. 105 (B3), 5783–5796.

Ablay, G.J., Martí, J., 2000. Stratigraphy, structure, and volcanic evolution of the Pico Teide–Pico Viejo formation, Tenerife, Canary Islands. J. Volcan. Geotherm. Res. 103 (1–4), 175–208.

Ablay, G.J., Ernst, G.G.J., Martí, J., Sparks, R.S.J., 1995. The −2 ka subplinian eruption of Montaña Blanca, Tenerife. Bull. Volcanol. 57 (5), 337–355.

Aki, K., Richards, P.G., 2002. Quantitative Seismology, 2nd edition. University Science Books.

Almendros, J., Ibáñez, J.M., Alguacil, G., Del Pezzo, E., 1999. Array analysis using circular-wave-front geometry: an application to locate the nearby seismo-volcanic source. Geophys. J. Int. 136 (1), 159–170.

Almendros, J., Ibáñez, J.M., Alguacil, G., Morales, J., Del Pezzo, E., La Rocca, M., Ortiz, R., Araña, V., Blanco, M.J., 2000. A double seismic antenna experiment at Teide volcano: existence of local seismicity and lack of evidences of volcanic tremor. J. Volcan. Geotherm. Res. 103 (1–4), 439–462.

Almendros, J., Chouet, B., Dawson, P., 2001. Spatial extent of a hydrothermal system at Kilauea Volcano, Hawaii, determined from array analyses of shallow long-period seismicity — 2. Results. J. Geophys. Res. 106 (B7), 13,581–13,597.

Almendros, J., Chouet, B., Dawson, P., Huber, C., 2002. Mapping the sources of the seismic wavefield at Kilauea Volcano, Hawaii, using data recorded on multiple seismic antennas. Bull. Seismol. Soc. Am. 92, 2333–2351.

Almendros, J., Luzón, F., Posadas, A., 2004. Microtremor analyses at Teide volcano (Canary Islands, Spain): assessment of natural frequencies of vibration using time-dependent horizontal-to-vertical spectral ratios. Pure Appl. Geophys. 161 (7), 1579–1596.

Antonioli, A., Piccinini, D., Chiaraluce, L., Cocco, M., 2005. Fluid flow and seismicity pattern: evidence from the 1997 Umbria–Marche (central Italy) seismic sequence. Geophys. Res. Lett. 32, L10311. doi:10.1029/2004GL022256.

Araña, V., Camacho, A.G., García, A., Montesinos, F.G., Blanco, I., Vieira, R., Felpeto, A., 2000. Internal structure of Tenerife (Canary Islands) based on gravity, aeromagnetic and volcanological data. J. Volcan. Geotherm. Res. 103 (1–4), 43–64.

Arciniega Ceballos, A., Chouet, B., Dawson, P., 2003. Long-period events and tremor at Popocatepetl volcano (1994–2000) and their broadband characteristics. Bull. Volcanol. 65, 124–135.

Battaglia, J., Got, J.L., Okubo, P., 2003. Location of long-period events below Kilauea Volcano using seismic amplitudes and accurate relative relocation. J. Geophys. Res. 108 (B12), 2553. doi:10.1029/2003JB002,517.

Benoit, J.P., McNutt, S.R., 1997. New constraints on source processes of volcanic tremor at Arenal volcano, Costa Rica, using broadband seismic data. Geophys. Res. Lett. 24 (4), 449–452.

Blanco, I. (1997), Análisis e interpretación de las anomalías magnéticas de tres calderas volcánicas: Decepción (Shetland del Sur, Antártida), Furnas (San Miguel, Azores) y Las Cañadas del Teide (Tenerife, Canarias), Ph.D. thesis, Universidad Complutense de Madrid.

Brodsky, E.E., Kanamori, H., 2001. The elastohydrodynamic lubrication of faults. J. Geophys. Res. 106, 16,357–16,374.

Caliro, S., Chiodini, G., Galluzzo, D., Granieri, D., La Rocca, M., Saccorotti, G., Ventura, G., 2005. Recent activity of Nisyros volcano (Greece) inferred from structural, geochemical, and seismological data. Bull. Volcanol. 67, 358–369. doi:10.1007/s00445-004-0381-7.

Canales, J.P., Dañobeitia, J.J., Watts, A.B., 2000. Wide-angle seismic constraints on the internal structure of Tenerife, Canary Islands. J. Volcan. Geotherm. Res. 103 (1–4), 65–81.

Canas, J.A., Ugalde, A., Pujades, L.G., Carracedo, J.C., Soler, V., Blanco, M.J., 1998. Intrinsic and scattering seismic wave attenuation in the Canary Islands. J. Geophys. Res. 103 (B7), 15,037–15,050.

Chouet, B., 1985. Excitation of a buried magmatic pipe; a seismic source model for volcanic tremor. J. Geophys. Res. 90 (B2), 1881–1893.

Chouet, B., 1986. Dynamics of a fluid-driven crack in three dimensions by the finite difference method. J. Geophys. Res. 91 (B14), 13,967–13,992.

Chouet, B., 1996. Long-period volcano seismicity; its source and use in eruption forecasting. Nature 380 (6572), 309–316.

Chouet, B., Page, R., Stephens, C., Lahr, J., Power, J., 1994. Precursory swarms of long-period events at Redoubt Volcano (1989–1990), Alaska; their origin and use as a forecasting tool. J. Volcan. Geotherm. Res. 62 (1–4), 95–135.

Del Pezzo, E., La Rocca, M., Ibáñez, J.M., 1997. Observations of high-frequency scattered waves using dense arrays at Teide volcano. Bull. Seismol. Soc. Am. 87 (6), 1637–1647.

Fernández, J., Yu, T.T., Rodríguez Velasco, G., González Matesanz, F.J., Romero, R., Rodríguez, G., Quirós, R., Dalda, A., Aparicio, A., Blanco, M.J., 2003. New geodetic monitoring system in the volcanic island of Tenerife, Canaries, Spain; combination of InSAR and GPS techniques. J. Volcan. Geotherm. Res. 124 (3–4), 241–253.

Ferreira, J.M., De Oliveira, R.T., Assumpção, M., Moreira, J.A.M., Pearce, R.G., Takeya, M.K., 1995. Correlation of seismicity and water level in the Açu reservoir — an example from northeast Brazil. Bull. Seismol. Soc. Am. 85, 1483–1489.

Frankel, A., 1994. Dense array recordings in the San Bernardino Valley of Landers–Big Bear aftershocks: basin surface waves, Moho reflections, and three-dimensional simulations. Bull. Seismol. Soc. Am. 84 (3), 613–624.

Fujita, E., Ida, Y., 2003. Geometrical effects and low-attenuation resonance of volcanic fluid inclusions for the source mechanism of long-period earthquakes. J. Geophys. Res. 108 (B2), 2118. doi:10.1029/2002JB001,806.

Fujita, E., Ida, Y., Oikawa, J., 1995. Eigen-oscillation of a fluid sphere and source mechanism of harmonic volcanic tremor. J. Volcan. Geotherm. Res. 69 (3–4), 365–378.

Fukao, Y., Fujita, E., Hori, S., Kanjo, K., 1998. Response of a volcanic conduit to step-like change in magma pressure. Geophys. Res. Lett. 25 (1), 105–108.

Galindo, I., Soriano, C., Martí, J., Pérez, N., 2005. Graben structure in the Las Cañadas edifice (Tenerife, Canary Islands): implications for active degassing and insights on the caldera formation. J. Volcan. Geotherm. Res. 144, 73–87.

Gil Cruz, F., Chouet, B., 1997. Long-period events, the most characteristic seismicity accompanying the emplacement and extrusion of a lava dome in Galeras Volcano, Colombia, in 1991. J. Volcan. Geotherm. Res. 77 (1–4), 121–158.

Hagerty, M.T., Schwartz, S.Y., Garcés, M.A., Protti, M., 2000. Analysis of seismic and acoustic observations at Arenal Volcano, Costa Rica, 1995–1997. J. Volcan. Geotherm. Res. 101 (1–2), 27–65.

Hellweg, M., 2000. Physical models for the source of Lascar's harmonic tremor. J. Volcan. Geotherm. Res. 101 (1–2), 183–198.

Hernández, P.A., Pérez, N.M., Salazar, J., Sato, M., Notsu, K., Wakita, H., 2000. Soil gas CO_2, CH_4, and H_2 distribution in and around Las Cañadas caldera, Tenerife, Canary Islands, Spain. J. Volcan. Geotherm. Res. 103 (1–4), 425–438.

Hernández, P.A., Pérez, N.M., Salazar, J., Ferrell, R., Álvarez, C., 2004. Soil volatile mercury, boron and ammonium distribution at Las Cañadas Caldera, Tenerife, Canary Islands, Spain. Appl. Geochem. 19 (6), 819–834.

Ibáñez, J.M., Del Pezzo, E., Almendros, J., La Rocca, M., Alguacil, G., Ortiz, R., García, A., 2000. Seismovolcanic signals at Deception Island volcano, Antarctica: wave field analysis and source modeling. J. Geophys. Res. 105 (B6), 13,905–13,931.

Iwamura, K., Kaneshima, S., 2005. Numerical simulation of the steam-water flow instability as a mechanism of long-period ground vibrations at geothermal areas. Geophys. J. Int. 163, 833–851.

Julian, B.R., 1994. Volcanic tremor: nonlinear excitation by fluid flow. J. Geophys. Res. 99 (B6), 11,859–11,877.

Kedar, S., Kanamori, H., Sturtevant, B., 1998. Bubble collapse as the source of tremor at Old Faithful Geyser. J. Geophys. Res. 103 (B10), 24,283–24,299.

Kumagai, H., Chouet, B., 2000. Acoustic properties of a crack containing magmatic or hydrothermal fluids. J. Geophys. Res. 105 (B11), 25,493–25,512.

Kumagai, H., Chouet, B.A., Nakano, M., 2002. Temporal evolution of a hydrothermal system in Kusatsu-Shirane Volcano, Japan, inferred from the complex frequencies of long-period events. J. Geophys. Res. 107 (B10), 2236. doi:10.1029/2001JB000653.

Lesage, P., Mora, M.M., Alvarado, G.E., Pacheco, J., Métaxian, J.-P., 2006. Complex behavior and source model of the tremor at Arenal volcano, Costa Rica. J. Volcanol. Geotherm. Res. 157 (1–3), 49–59. doi:10.1016/j.jvolgeores.2006.03.047.

Martí, J., Gudmundsson, A., 2000. The Las Cañadas Caldera (Tenerife, Canary Islands); an overlapping collapse caldera generated by magma-chamber migration. J. Volcan. Geotherm. Res. 103 (1–4), 161–173.

Martí, J., Mitjavila, J., Araña, V., 1994. Stratigraphy, structure and geochronology of the Las Cañadas caldera (Tenerife, Canary Islands). Geol. Mag. 131, 715–727.

Métaxian, J.-P., Lesage, P., Valette, B., 2002. Locating sources of volcanic tremor and emergent events by seismic triangulation: application to Arenal volcano, Costa Rica. J. Geophys. Res. 107 (B10), 2243. doi:10.1029/2001JB000559.

Métaxian, J.-P., O'Brien, G.S., Bean, C.J., Mora, M., 2006. Seismic wave simulation on Arenal Volcano (Costa Rica): evidence of topographic effects. Geophys. Res. Abstr. 8, 03089.

Mezcua, J., Buforn, E., Udías, A., Rueda, J., 1992. Seismotectonics of the Canary Islands. Tectonophysics 208, 447–452.

Neuberg, J., Luckett, R., Baptie, B., Olsen, K., 2000. Models of tremor and low-frequency earthquake swarms on Montserrat. J. Volcan. Geotherm. Res. 101 (1–2), 83–104.

Noir, J., Jacques, E., Bekri, S., Adler, P.M., Tapponier, P., King, G.C.P., 1997. Fluid flow triggered migration of events in the 1989 Dobi earthquake sequence of central Afar. Geophys. Res. Lett. 24, 2335–2338.

Ortiz, R., Araña, V., Astiz, M., García, A., 1986. Magnetotelluric study of the Teide (Tenerife) and Timanfaya (Lanzarote) volcanic areas. J. Volcan. Geotherm. Res. 30 (3–4), 357–377.

Ortiz, R., Moreno, H., García, A., Fuentealba, G., Astiz, M., Na, P.P., Sánchez, N., Tárraga, M., 2003. Villarrica volcano (chile): characteristics of the volcanic tremor and forecasting of small explosions by means of a material failure method. J. Volcan. Geotherm. Res. 128 (1–3), 247–259.

Pérez, N.M., Nakai, S., Wakita, H., Pacheco, A.H., Salazar, J.M., 1996. Helium-3 emission in and around Teide Volcano, Tenerife, Canary Islands, Spain. Geophys. Res. Lett. 23 (24), 3531–3534.

Pérez, N.M., Melían, G., Galindo, I., Padrón, E., Hernández, P.A., Nolasco, D., Salazar, P., Pérez, V., Coello, C., Marrero, R., González, Y., González, P., Barrancos, J., 2005. Premonitory geochemical and geophysical signatures of volcanic unrest at Tenerife, Canary Islands. Geophys. Res. Abstr. 7, 09993.

Pous, J., Heise, W., Schnegg, P.A., Muñoz, G., Martí, J., Soriano, C., 2002. Magnetotelluric study of the Las Cañadas Caldera (Tenerife, Canary Islands); structural and hydrogeological implications. Earth Planet. Sci. Lett. 204, 249–263.

Powell, T.W., Neuberg, J., 2003. Time dependent features in tremor spectra. J. Volcan. Geotherm. Res. 128 (1–3), 177–185.

Power, J.A., Stihler, S.D., White, R.A., Moran, S.C., 2004. Observations of deep long-period (DLP) seismic events beneath Aleutian arc volcanoes; 1989–2002. J. Volcan. Geotherm. Res. 138, 243–266.

Saccorotti, G., Ventura, G., Vilardo, G., 2002. Seismic swarms related to diffusive processes: the case of Somma-Vesuvius volcano, Italy. Geophysics 67 (1), 199–203.

Saccorotti, G., Zuccarello, L., Del Pezzo, E., Ibáñez, J.M., Gresta, S., 2004. Quantitative analysis of the tremor wavefield at Etna Volcano, Italy. J. Volcan. Geotherm. Res. 136, 223–245.

Sevilla, M.J., Romero, P., 1991. Ground deformation control by statistical analysis of a geodetic network in the caldera of Teide. J. Volcan. Geotherm. Res. 65–74.

Shapiro, S.A., Huenges, E., Borm, G., 1997. Estimating the crust permeability from fluid-injection-induced seismic emission at the KTB site. Geophys. J. Int. 131, F15–F18.

Shapiro, S.A., Audigane, P., Royer, J.J., 1999. Large-scale in situ permeability tensor of rocks from induced seismicity. Geophys. J. Int. 137, 207–213.

Shapiro, S.A., Patzig, R., Rothert, E., Rindschwentner, J., 2003. Triggering of seismicity by pore-pressure perturbations: permeability-related signatures of the phenomenon. Pure Appl. Geophys. 160, 1051–1066.

Soler, V., Castro Almazán, J.A., Viñas, R.T., Eff-Darwich, A., Sánchez Moral, S., Hillaire Marcel, C., Farrujia, I., Coello, J., De La Nuez, J., Martín, M.C., Quesada, M.L., Santana, E., 2004. High CO_2 levels in boreholes at El Teide volcano complex (Tenerife, Canary Islands): implications for volcanic activity monitoring. Pure Appl. Geophys. 161, 1519–1532.

Soosalu, H., Lippitsch, R., Einarsson, P., 2006. Low-frequency earthquakes at the Torfajökull volcano, south Iceland. J. Volcan. Geotherm. Res. 153, 187–199.

Takagi, N., Kaneshima, S., Kawakatsu, H., Yamamoto, M., Sudo, Y., Ohkura, T., Yoshikawa, S., Mori, T., 2006. Apparent migration of tremor source synchronized with the change in the tremor amplitude observed at Aso volcano, Japan. J. Volcan. Geotherm. Res. 154, 181–200.

Talwani, P., Acree, S., 1984. Pore pressure diffusion and the mechanism of reservoir-induced seismicity. Pure Appl. Geophys. 122 (6), 947–965.

Talwani, P., Cobb, J.S., Schaeffer, M.F., 1999. In situ measurements of hydraulic properties of a shear zone in northwestern South Carolina. J. Geophys. Res. 104, 14,993–15,004.

Ukawa, M., 2005. Deep low-frequency earthquake swarm in the mid crust beneath Mount Fuji (Japan) in 2000 and 2001. Bull. Volcanol. 68, 47–56.

Watts, A.B., 1994. Crustal structure, gravity anomalies and flexure of the lithosphere in the vicinity of the Canary Islands. Geophys. J. Int. 119, 648–666.

Yu, T.T., Fernández, J., Tseng, C.L., Sevilla, M.J., Araña, V., 2000. Sensitivity test of the geodetic network in Las Cañadas Caldera, Tenerife, for volcano monitoring. J. Volcan. Geotherm. Res. 103, 393–407.